



Electrochromism in copper oxide thin films

T.J. Richardson *, J.L. Slack, M.D. Rubin

Environmental Energy Technologies Division, Ernest Orlando Lawrence Berkeley National Laboratory, Berkeley, CA 94720, USA

Received 23 August 2000

Abstract

Transparent thin films of copper(I) oxide prepared on conductive SnO₂/F glass substrates by anodic oxidation of sputtered copper films or by direct electrodeposition of Cu₂O transformed reversibly to opaque metallic copper films when reduced in alkaline electrolyte. In addition, the same Cu₂O films transform reversibly to black copper(II) oxide when cycled at more anodic potentials. Copper oxide-to-copper switching covered a large dynamic range, from 85 to 10% photopic transmittance, with a coloration efficiency of about 32 cm²/C. Gradual deterioration of the switching range occurred over 20–100 cycles. This is tentatively ascribed to coarsening of the film and contact degradation caused by the 65% volume change on conversion of Cu to Cu₂O. Switching between the two copper oxides (which have similar volumes) was more stable and more efficient (CE = 60 cm²/C), but covered a smaller transmittance range (60–44% *T*). Due to their large electrochemical storage capacity and tolerance for alkaline electrolytes, these cathodically coloring films may be useful as counter electrodes for anodically coloring electrode films such as nickel oxide or metal hydrides. Published by Elsevier Science Ltd.

Keywords: Electrochromism; Copper; Copper oxide; Thin films; Electrochemical switching

1. Introduction

The anodic formation and complex electrochemical properties of copper oxide films on bulk copper electrodes in alkaline electrolytes have been studied extensively [1–7]. While there is some controversy surrounding the precise sequence of compounds produced on the electrode surface, it is clear that copper(I) oxide, Cu₂O, is produced, followed by copper(II) oxide, CuO. Due to the poor electronic conductivity of stoichiometric Cu₂O, the two oxides can coexist with copper. The oxide films can persist only within a narrow pH range [8]. Both oxides are semiconductors, Cu₂O having a direct bandgap of about 2.1 eV [9,10], and therefore strongly absorbing at wavelengths below 600 nm, with a reddish appearance. CuO, with $E_g = 1.3$ [11], is absorbing throughout the visible spectrum.

While thin Cu₂O films with high transparency can easily be made by a variety of routes, and electrochromic behavior has been reported [12–14] on lithium intercalation of Cu_xO films, electrochromic devices based on interconversion of Cu and Cu₂O, or of Cu₂O and CuO do not appear to have been investigated. Unlike electrochromic devices based on reflective metal films (typically bismuth or silver) that are alternately deposited and stripped, the present system involves transformations from metal to oxides in an intact film.

2. Experimental

All films were deposited on SnO₂/F coated glass substrates. Metallic copper films were prepared by DC magnetron sputtering from an oxygen-free high conductivity Cu target in an argon atmosphere at a pressure of 10 mTorr. The typical base pressure was

* Corresponding author. Tel/fax.: +1-510-4868619.

E-mail address: tjrichardson@lbl.gov (T.J. Richardson).

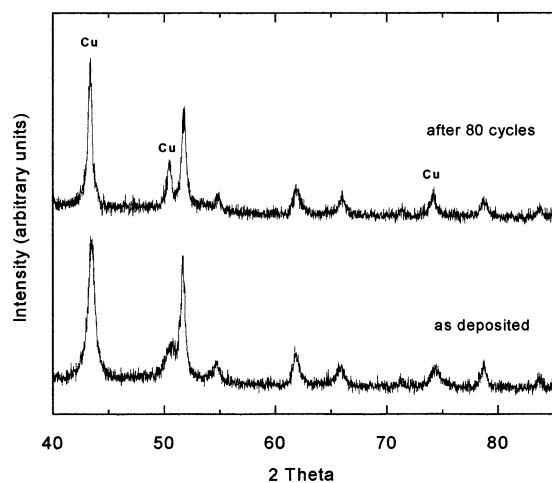


Fig. 1. XRD patterns of sputter-deposited copper films on SnO_2/F glass. Unlabelled peaks are due to SnO_2/F .

2.0×10^{-6} Torr; with applied power of 100 W, a 30 nm film was deposited in 3 min. Cu_2O films were prepared by DC magnetron reactive sputtering using the same

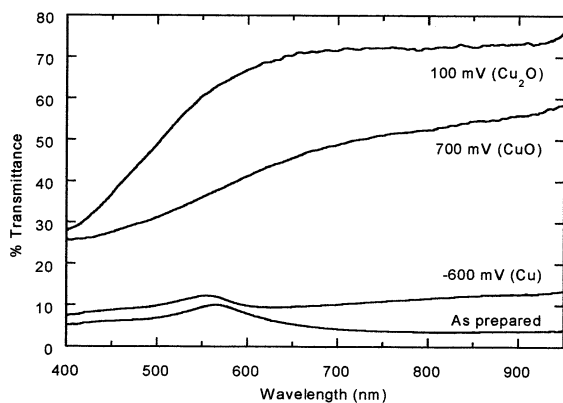


Fig. 2. Visible transmittance spectra obtained in situ during electrochemical cycling of copper/copper oxide films.

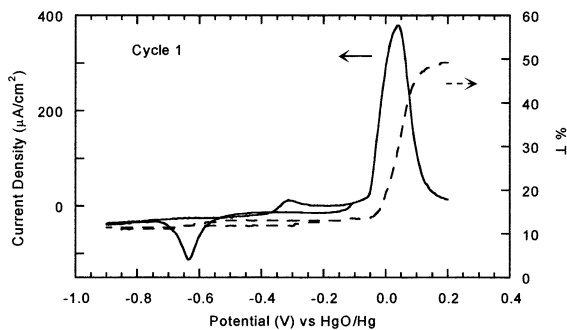


Fig. 3. First cathodic and anodic sweeps for 40 nm sputtered copper film (1 mV/s, 0.1 M NaOH).

target. Ar (99.9995%) was delivered through the sputter gun, across the target surface at 240 sccm. The O_2 (99.998%) flow rate was 5.3 sccm, directed at the substrate from below. The total process pressure was 21.3 mTorr, with oxygen partial pressure estimated to be between 1.0 and 1.5 mTorr. Copper oxide films also were electrodeposited from alkaline copper sulfate/lactic acid solutions according to the method of Mukhopadhyay et al. [15]. Film thicknesses were measured by profilometry (Dektak). Electrochemical oxidation and cycling of films were carried out in a 50 ml fused silica cuvette containing 0.1 M NaOH electrolyte, using a platinum foil counter electrode and an HgO/Hg reference electrode (Radiometer). Photopic transmittance was monitored by an International Light silicon detector with output coupled to the computerized potentiostat/galvanostat (Arbin, Inc.). Visible spectra were recorded using a fiber optic spectrometer (Ocean Optics). X-ray diffraction (XRD) patterns of films as deposited and after cycling were obtained using a Siemens thin film diffractometer with an incident beam angle of 0.5° from the sample surface.

3. Results

XRD patterns obtained from a freshly prepared, 40 nm thick copper film (Fig. 1, trace a) contained strong peaks due to metallic Cu and the underlying SnO_2/F layer. Some very weak reflections due to Cu_2O can be discerned. The crystallite size, estimated from the peak width, is 12 nm. The visible transmission spectrum of this sample, uncorrected for the substrate, is shown in Fig. 2 (bottom trace). The presence of a native oxide layer on the surface of the copper films inhibited the anodic conversion of Cu to Cu_2O unless it was first reduced by sweeping cathodically to -900 mV (Fig. 3). A slight decrease in transmittance accompanied the reduction peak at -0.63 V. On the first anodic sweep, copper was oxidized to Cu_2O at 0.05 V, with rapid bleaching of the film. Subsequent cycles were similar to that shown in Fig. 4, except that the height of the peaks increases over the first three or four cycles, with a corresponding increase in the optical switching range. Reduction to copper metal takes place beginning at -0.4 V, becoming rapid at -0.8 V. The shape of the reduction curve strongly suggests a nucleation mechanism. The re-oxidation of the copper film proceeds in three distinct steps at -0.3 , 0.0, and 0.2 V. Bleaching of the film occurs at each step, but with coloration efficiencies of 54, 29, and 35 cm^2/C , respectively. The recovered Cu film is somewhat more crystalline (est. size 20 nm) than the initial deposit.

Visible transmission spectra of this electrode in the three different states are presented in Fig. 2. In the

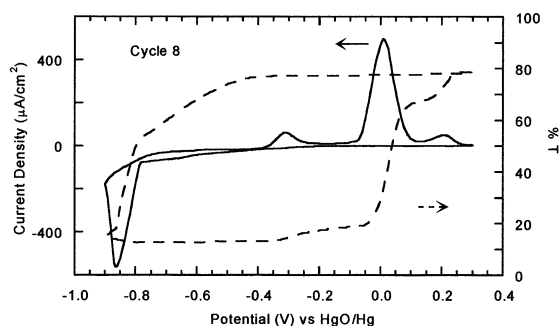


Fig. 4. Eighth cycle, same electrode and conditions as in Fig. 3.

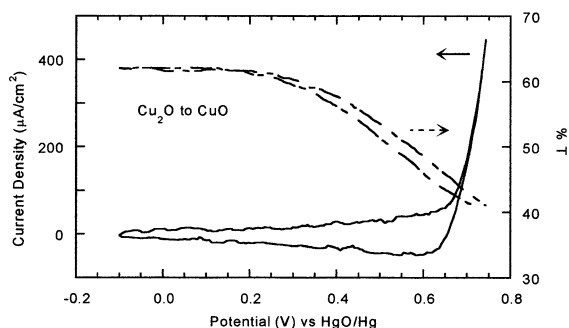


Fig. 5. High potential region (1 mV/s, 0.1 M NaOH).

Cu_2O state, the film is quite clear and only slightly yellow in appearance. The copper state obtained by reduction of this oxide is not as reflecting as the original sputtered film, but is still mirror-like. The highest quality copper state was found after polarizing the electrode at -0.6 V for an extended period, rather

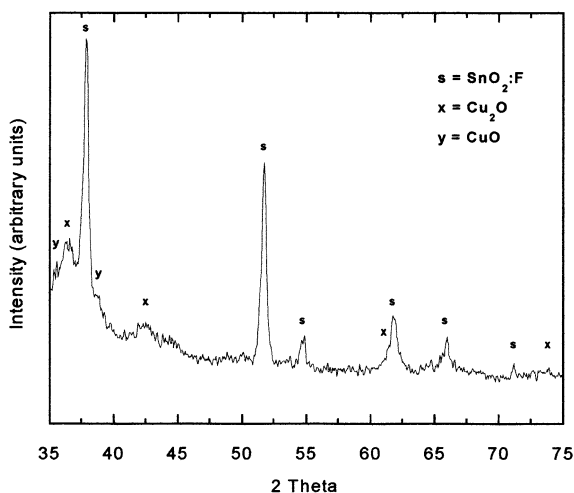


Fig. 6. XRD pattern of electrode from Fig. 5.

than sweeping rapidly to more negative potentials. The dark state produced by anodic polarization, referred to as “ CuO ”, begins to appear at 0.2 V (Fig. 5). Despite the black color of CuO , the switching here is limited to about 20%. Polarization beyond 0.7 V resulted in oxygen evolution and no further darkening of the film. An XRD pattern obtained from this electrode (Fig. 6), removed from the electrolyte in its darkest state, shows the poorly crystalline nature of the copper oxide layer. The very weak reflections due to CuO are discernable, with somewhat stronger reflections from Cu_2O .

Sputtered Cu_2O films contained small amounts of Cu and had a deep copper color. Oxidation following reduction of the entire film to copper produced a clear, highly transparent, and strongly adherent Cu_2O film, which exhibited superior cycling stability to the mainly metallic precursor films described above. Electrodeposited Cu_2O was less uniform and adherent, but could be cycled several times over a wide range of visible transmittance.

4. Discussion

The electrochemical behavior of these copper/copper oxide films and the phases present at different potentials are consistent with results for bulk copper in similar electrolytes [1–7]. In the latter case, however, continuing oxidation of the underlying copper causes some overlapping of anodic peaks. The absence of cathodic features prior to Cu_2O reduction to Cu in our experiments (but seen on bulk copper) may be due to the low conductivity of Cu_2O . It is not until dendrites of Cu have begun to penetrate the oxide that reduction can proceed at a significant rate. The nucleation and dendritic growth of Cu from the oxide may also account for the coarsening of the metallic copper film relative to the original. Poor conductivity in Cu_2O may also contribute to the difficulty of converting it to CuO at higher potentials.

Dissolution of copper species in the electrolyte does not appear to play a significant role in the electrochromic processes described here. Extensive dissolution would result in irreversible loss of copper due to the large quantity (40 ml) of electrolyte and small electrode area ($5\text{--}6\text{ cm}^2$). In addition, redistribution of material over the surface was not observed, and portions of the film at different distances from the counter electrode behaved identically. Nor were deposits observed to accumulate on the counter electrode.

Crystalline metallic copper contains 85 Cu atoms/ nm^3 [16]. In Cu_2O , there are 52 Cu atoms/ nm^3 [17], corresponding to a volume expansion on forming the oxide of 65%. This expansion and contraction eventually fractures the film and, along with the coarsening of

the particles, reduces its reflectivity in the metallic state, while increasing the transparency of the oxide states. This may help to explain the relative stability of sputtered $\text{Cu}_2\text{O}(\text{Cu})$ films, which have an intermediate original volume. Conversion of Cu_2O to CuO (49 atoms/ nm^3 [18]), however, involves little volume change and minimal rearrangement of the structure. This, combined with the inability to completely interconvert the two oxides, may contribute to the good cyclability in the high potential region. Interestingly, the intermediate Cu(I) , Cu(II) oxide, Cu_4O_3 [19], does not appear to be formed during oxidation of Cu_2O .

The oxidation of copper to Cu_2O in three steps is intriguing. The first peak (-0.3 V) appears during oxidation of bulk copper, and has been attributed to formation of a surface oxide layer. Its magnitude, however, increases somewhat as the copper particles become larger. This step represents about 12% of the total charge required to reach the maximum transparency. Some lower oxides of copper, designated Cu_8O and Cu_4O , have been observed by electron diffraction on partially oxidized copper surfaces. It is possible that formation of an intermediate lower oxide is responsible for this feature. In situ XRD experiments are planned to investigate the nature of these three steps.

5. Conclusions

The copper-to-copper oxide transition reveals a new, cathodically coloring, electrochromic system, which combines a highly reflecting metallic state with a highly transparent insulating state. Devices pairing it with passive or anodically coloring counter electrodes (such as nickel oxide or a hydride mirror electrode) may offer a unique range of transmitting and reflecting states. The copper(I)-to-copper(II) oxide transition may also be useful in such a device or, given improvements in the switching range, may find its own applications.

Acknowledgements

This work was supported by the Assistant Secretary for Energy Efficiency and Renewable Energy, Office of Building Technologies, Building Systems and Materials Division of the US Department of Energy under Contract No. DE-AC03-76SF00098. The authors thank Dr Robert Kostecki of LBNL for helpful discussions.

References

- [1] H.Y.H. Chan, C.G. Takoudis, M.J. Weaver, *J. Phys. Chem. B* 103 (1999) 357.
- [2] S. Hartinger, B. Pettinger, K. Doblhofer, *J. Electroanal. Chem.* 397 (1995) 335.
- [3] W. Kautek, J.G. Gordon, *J. Electrochem. Soc.* 137 (1990) 2672.
- [4] J.C. Hamilton, J.C. Farmer, R.J. Anderson, *J. Electrochem. Soc.* 133 (1986) 739.
- [5] S.T. Mayer, R.H. Muller, *J. Electrochem. Soc.* 139 (1992) 426.
- [6] B. Miller, *J. Electrochem. Soc.* 116 (1969) 1675.
- [7] J.L. Ord, D.J. DeSmet, Z.Q. Huang, *J. Electrochem. Soc.* 134 (1987) 826.
- [8] B. Beverskog, I. Puigdomenech, *J. Electrochem. Soc.* 144 (1997) 3476.
- [9] T.D. Golden, M.G. Shumsky, Y. Zhou, R.A. NanderWerf, R.A. Van Leeuwen, J.A. Switzer, *Chem. Mater.* 8 (1996) 2499.
- [10] M.T.S. Nair, L. Guerrero, O.L. Arenas, P.K. Nair, *Appl. Surf. Sci.* 150 (1999) 143.
- [11] F. Marabelli, G.B. Parravicini, F. Salghetti-Drioli, *Phys. Rev. B* 52 (1995) 1433.
- [12] N. Ozer, F. Tepehan, *Sol. Energy Mater. Sol. Cells* 30 (1993) 13.
- [13] H. Demiryont, US Patent 4,830,471.
- [14] F.I. Brown, S.C. Schulz, US Patent 5,585,959.
- [15] A.K. Mukhopadhyay, A.K. Chakraborty, A.P. Chatterjee, S.K. Lahiri, *Thin Solid Films* 209 (1992) 92.
- [16] H.E. Swanson, E. Tatge, US NBS Circular 359 (1953) 1.
- [17] R. Restori, D. Schwarzenbach, *Acta Crystallogr. B* 42 (1986) 201.
- [18] S. Asbrink, L.J. Lorrby, *Acta Crystallogr. B* 26 (1970) 8.
- [19] M. O'Keefe, J.O. Bovin, *Am. Miner.* 63 (1978) 180.